Photon Upconversion in the Visible Wavelengths with ZnSe/InP/ZnS Nanocrystals

Paulina Jaimes[a+], Tsumugi Miyashita[b+], Tian Qiao[a], Kefu Wang[a], and Ming Lee Tang[a, b*]
[a]Department of Chemistry, University of Utah, Salt Lake City, UT, 84112, United States.
[b]Department of Biomedical Engineering, University of Utah, Salt Lake City, UT, 84112, United States.
[+]Authors contributed equally

Corresponding author's email:
Minglee.tang@utah.edu

Abstract
Nanocrystals that can absorb strongly in the near-infrared (NIR) wavelengths for conversion to visible light are of great interest for biological imaging applications. In this work, we examine an inverse-Type I heterostructure with an inner InP shell for triplet-triplet annihilation based photon upconversion. InP-based nanocrystals are earth-abundant, benign, and can be synthetically tuned to absorb in the entire NIR window I. Here, a two monolayer ZnS shell was used to passivate the surface defects on inverse Type-I ZnSe/InP core/shell particles. We show that this ZnS shell increases the InP photoluminescence quantum yield (QY) by a factor of 16 to 0.43 and the transmitter triplet lifetime from 138 μs to 451 μs, but decreases the rate of triplet energy transfer by a factor of 3. This results in the ZnSe/InP and ZnSe/InP/ZnS nanocrystal triplet photosensitizers producing a similar photon upconversion QY of about 4.0% (out of a maximum of 50%) when paired with 9,10-diphenylanthracene as the blue emitter. This work suggests that the ZnS shell can be further tuned to increase the photon upconversion QY. This work also shows that ZnSe/InP/ZnS nanocrystals are promising candidates for hybrid organic-inorganic nanostructure that can convert NIR photons to visible light.

Introduction
InP nanocrystals (NCs) are attractive for consumer applications because they are environmentally friendly especially when compared to heavy-metal containing quantum dots (QDs). As a result, InP based NCs are used in displays even though higher color purity can be more easily achieved with cadmium chalcogenide NCs.(1-7) The relative safety of indium based NCs has motivated research into the utilization of InP and InAs NCs as bioimaging probes.(8, 9) InP NCs can absorb in the first biological window where there is minimal light scattering and absorption seen by endogenous molecules.(9-11) Similarly, the use of InP QDs for photon upconversion *in-vivo* would eliminate toxicity concerns while allowing new applications in optogenetics, two-photon imaging, phototherapy, etc.

Pure InP NCs and type-I InP/ZnSe/ZnS NCs have been used as triplet photosensitizers for the conversion of blue to ultra-violet and green to blue light respectively. Zhang and Castellano used small InP NCs with the first excitonic absorption maxima at 410 nm to photosensitize the triplet state of 2,5-diphenyloxazole (PPO), to obtain a normalized photon upconversion QY of 3.7% (Φ_{NUCPL}= 3.7% where 100% is the maximum).(12) Lai and Wu used larger InP NCs for triplet photosensitization.(13) While they did not observe photon upconversion with pure InP NCs, InP/ZnSe/ZnS NCs with an absorption peak at 540nm were successfully used to convert excitation at 530 nm and 590 nm to blue emission. This photon upconversion was a result of triplet-triplet annihilation (TTA) by 9,10-diphenylanthracene (DPA) for Φ_{NUCPL}= 10.0%. Both studies reported high triplet energy transfer efficiencies: 84% for Lai et al, and nearly 100% for Zhang and co-workers. Triplet energy transfer time constants of 1−4 nanoseconds to surface bound anthracene, naphthalene, and quinoline molecules were observed regardless of whether the InP NCs had a zinc chalcogenide shell. This is unexpected because the Type I band structure created from a ZnSe/ZnS shell should result in a tunneling barrier for exciton transfer from the InP core to molecular triplet acceptors on the NC surface. This tunning barrier is expected to decrease the rate of triplet energy transfer

(TET). In addition, it is strange that this ns TET time constant to anthracene from core-only InP is almost an order of magnitude slower compared to TET from pure CdSe, given that the driving force is similar. It is also interesting to note that the triplet sensitizing state from small InP NCs with absorption maxima at 410nm varies with the molecular acceptor. By fitting temperature dependent PL to a model invoking thermally activated delayed photoluminescence between InP and the molecular acceptor, Zhang et al concluded that the energy gap between the dark exciton in InP NCs and molecular triplet state is pinned at ~0.10 eV. This is because their model invokes reversible TET even though the acceptor molecule level varies from 2.46 eV to 2.62 eV. These reports warrant further investigation into InP NCs with alternative core-shell geometries. A better understanding of the structure-property relationships will enable the efficient photosensitization of molecular triplet states by InP NCs for photon upconversion.

Here, inverse Type-I heterostructure ZnSe/InP/ZnS NCs are examined for their potential to absorb near-infrared (NIR) photons. The ultimate goal is the conversion of NIR to visible light via TTA. The Dennis group has shown that these NCs absorb strongly in the first NIR optical tissue window, with first absorption maxima up to 845 nm.(9) In contrast, the most red-shifted absorption maxima for pure InP, InP/ZnS, or InP/ZnSe NCs is 655 nm.(14-17) It is challenging to synthesize InP based NCs that can absorb up to the InP bulk bandgap of 1.35 eV or 919 nm. Comparing ZnSe/InP to ZnSe/InP/ZnS NCs that absorb in the green, we confirm that the ZnS shell does passivate the NC surface, just like it does for CdS and PbS NCs.(18-20) While this two-monolayer thick ZnS increases the NC lifetime, surface bound molecular triplet lifetime and the band edge emission, it does not improve the photon upconversion QY. This is because the rate of TET transfer from NC to the molecular transmitter slows down by a factor of 3 in the presence of this ZnS shell. Nevertheless, this work shows that these direct gap ZnSe/InP/ZnS NCs can provide a viable route for the photon upconversion of NIR to visible photons.

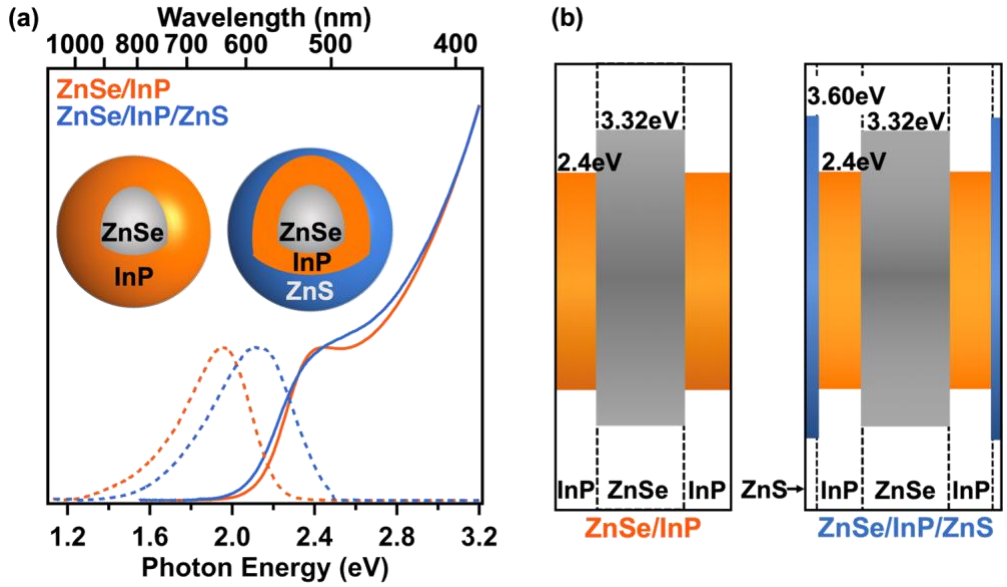

Figure 1. (a) Normalized absorption (solid) and emission (dashed) spectra of both samples, ZnSe/InP (orange) and ZnSe/InP/ZnS (blue). (b) The band gap alignment of ZnSe/InP and ZnSe/InP/ZnS QDs that both contain a ZnSe core with diameter of 2.50nm.

Table 1. Key parameters for ZnSe/InP and ZnSe/InP/ZnS QDs

Sample	λ_{abs}[a] (nm)	HWHM (nm)	λ_{em}[b] (nm)	HWHM (nm)	PLQY[c] (%)	$\langle k_r \rangle$[d] (s^{-1})	$\langle \tau \rangle$[e] (ns)	$\langle \tau \rangle_{9\text{-ACA}}$[f] (ns)
ZnSe/InP	508	44	635	79	2.95	6.6×10^5	44.2	5.15

ZnSe/InP/ZnS	508	-	579	81	43.34	3.1×10^6	138	16.3

[a]First exciton absorption maxima. [b]Emission peak when excited with a 488nm CW laser. [c]Reference for the photoluminescence QY is taken by 4-(Dicyanomethylene)-2-methyl-6-(4-dimethylaminostyryl)-4H-pyran (DCM), which has a fluorescence QY of 30% in methanol. [d]$\langle k_r \rangle$ is the radiative decay rate of the NCs. [e, f]$\langle \tau \rangle$ and $\langle \tau \rangle_{9\text{-ACA}}$ indicate the lifetimes of the NCs with and without 9-ACA. All measurements were at RT in toluene.

Methods

When choosing an InP NC light absorber for photon upconversion based on triplet-triplet annihilation, we examined published work to find a structure that would be able to photosensitize the lowest triplet excited state of perylene or anthracene at 1.53 and 1.8 eV respectively.(21) We started with the seedless variable rate injection method introduced by Achorn et al(22) because their red absorbing core/shell InP/ZnSe structures seemed very promising for the conversion of NIR to visible photons. Unfortunately, in our hands, the UCQY was less than 0.10% (data not shown). We then looked at the Cossiart's group InP/ZnSe NCs, using tris-diethylaminophosphine as a phosphorous precursor(23), but unfortunately these triplet photosensitizers also resulted in systems with a low UCQY (data not shown).

We settled on a ZnSe/InP/ZnS nanostructure that was reported to have a high PLQY and absorption in the NIR.(9) Two InP-based NCs, one with a core/shell structure and a second one with a core/shell/shell structure were synthesized for this study using air-free conditions based on methods introduced by Peng and Dennis.(24) The first InP NC sample contains a ZnSe core with a diameter of 2.50 nm (as determined by the first exciton absorption maxima in Figure S1 in the supporting information, SI). It has a 3 monolayer (ML) InP shell on it, as shown by inductively coupled plasma mass spectroscopy (ICP-MS) (Table S1 and S2 in the SI). This creates an inverse Type-I heterostructure. The second sample contains the same ZnSe/InP core/shell and a second two monolayer thick ZnS shell, giving it a core/shell/shell structure, as shown by ICP-MS (Table S1 and S2 in the SI). It is essential to cool the core/shell structure quickly after growing the InP MLs on the ZnSe core. We found that the core/shell ZnSe/InP NCs has a broad emission peak with a noticeable trap state if cooling were allowed to occur naturally. In contrast, a faster cooling process with compressed air resulted in more well-defined, sharper emission spectra with virtually no trap state (see Figure S2 in the SI).

Results

Figure 1a shows the normalized electronic absorption and photoluminescence (PL) data of both samples. The Dennis group found that an InP shell >0.5 nm localizes the heavy hole of the InP on the InP shell regardless of the ZnSe core size or ZnS shell thickness. This in turn allows the InP shell thickness to dictate the absorption and emission spectra. From Figure 1a, going from ZnSe/InP to ZnSe/InP/ZnS, the first absorption maxima broadens, loses the excitonic fine structure and red shifts at its tail. This suggests that growth of the ZnS shell increases sample inhomogeneity and broadens nanoparticle size distribution. Thus, an optical absorption gap of 2.4 eV is drawn for both samples for the InP shell in the energy diagram in Fig. 1b. The ZnSe/InP NC sample shows a sharper emission peak than that of the ZnSe/InP/ZnS sample (Figure S3 in the SI). A blue shift is seen in the ZnSe/InP/ZnS emission spectra compared to its ZnSe/InP core, possibly due to the formation of an alloy at the interface between the InP and ZnS that confines the exciton relative to the original core. The transmission electron micrograph of this ZnSe/InP/ZnS sample can be seen in Figure S4. Previously published results on an InP/ZnSe core/shell structure show a notable rise in the absorption spectra above 2.75 eV corresponding to the ZnSe shell composed of 6-7 MLs.(25) This is not observed in this work because because our ZnS shell here is only 2 ML thick as shown by inductively coupled plasma mass spectrometry (ICP-MS). The optical profiles of each sample are summarized in Table 1. Note that the broad PL linewidths of InP compared to CdSe are assigned to electron-phonon coupling.(25, 26)

InP is known to be sensitive to oxidation and surface defects. This results in poor emission and a low PLQY. The exciton is inadvertently quenched by trap states that arise from surface defects/ lattice distortions/ structural disorder resulting in hole localization. The ZnS shell here is one way to address susceptibility to surface defects and improve the NC PLQY. 4-(Dicyanomethylene)-2-methyl-6-(4-dimethylaminostyryl)-4H-pyran in methanol was used as a PLQY standard to match the red emission of the NCs (see the SI for more details). Using this, the band edge PLQY of ZnSe/InP was found to be 2.95% while the shelled ZnSe/InP/ZnS had a PLQY of 43.34%. As reported in literature, adding a protective shell over the InP NC passivates trap states and improves the PLQY.(27) Nanosecond transient absorption (ns-TA) spectroscopy was used to quantify the changes in the elementary exciton decay processes resulting from the ZnS shell (Figure 2). In order to calculate the radiative decay rate after the ZnS shell growth, the ground state bleach (GSB) at 500-510 nm attributed to InP was fit with three exponentials (Fig. 3, S5 and Table S3). The amplitude weighted average lifetime of the NCs, τ, increases from 44.3 ns to 138 ns with the ZnS shell. As can be seen in Table 1, the ZnS shell increases the radiative decay rate, k_r, by an order of magnitude, confirming that the shell growth passivates surface trap states, increasing the PLQY (see SI section 4).

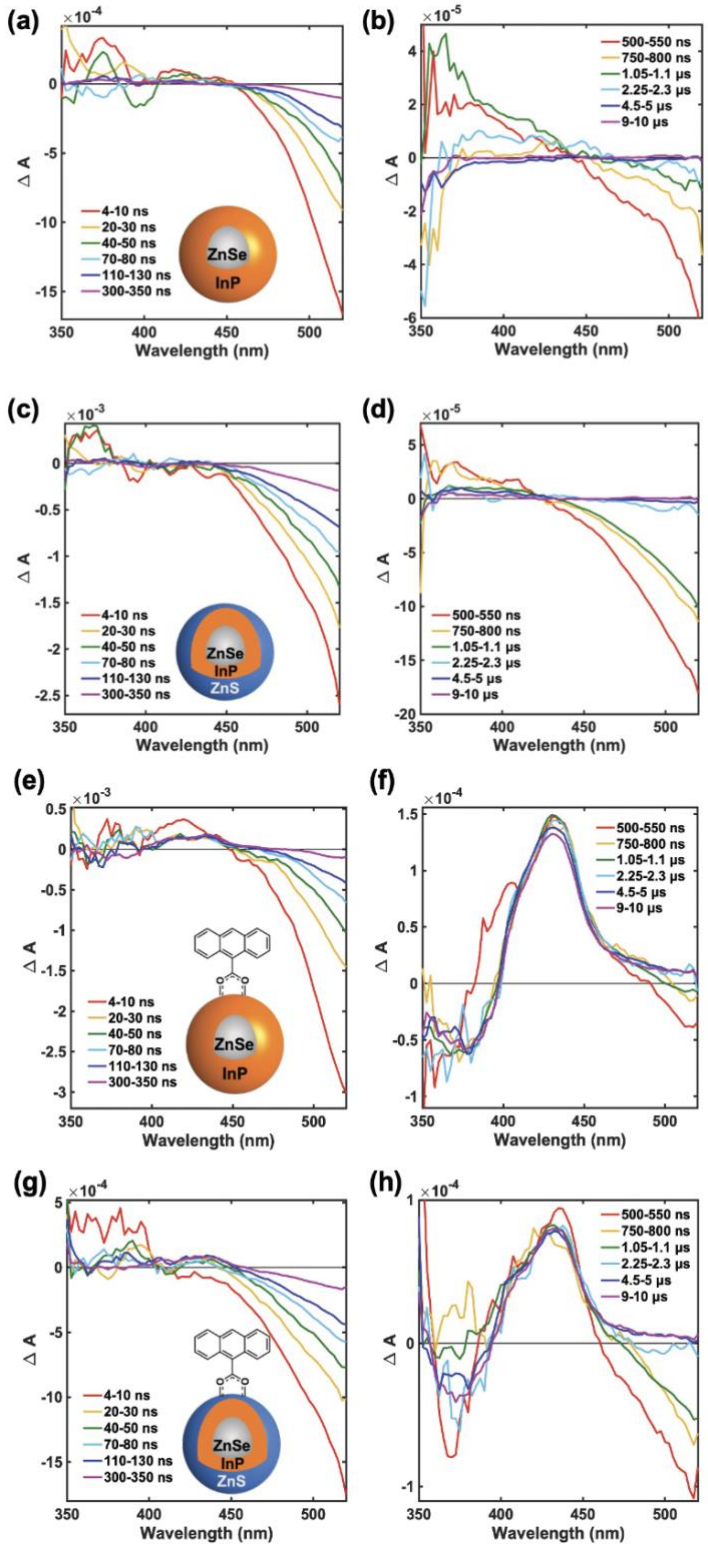

Figure 2. Transient absorption (TA) spectra at 4–350 ns for (a) ZnSe/InP, (c) ZnSe/InP/ZnS, (e) ZnSe/InP//9-ACA and (g) ZnSe/InP/ZnS//9-ACA and at 500 ns–10 µs for (b) ZnSe/InP, (d) ZnSe/InP/ZnS, (f) ZnSe/InP//9-ACA and (h) ZnSe/InP/ZnS//9-ACA. All samples are in toluene excited at 532 nm at RT.

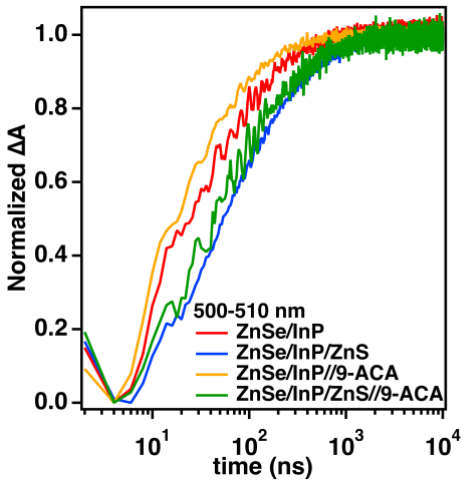

Figure 3. Transient kinetics of ZnSe/InP (red), ZnSe/InP/ZnS (blue), ZnSe/InP//9-ACA (orange) and ZnSe/InP/ZnS//9-ACA (green) at 500-510 nm.

The maximum photon upconversion QY, Φ_{NUCPL}, for ZnSe/InP and ZnSe/InP/ZnS is 4.16 % and 4.00% respectively when paired with 9,10-diphenylanthracene (DPA) as the triplet annihilator (Table 2). Here, 50% is defined as the maximum theoretical value of UCQY because of the two-to-one nature of TTA based photon upconversion. This Φ_{NUCPL} is 1.5 times lower than the best values for PbS QD triplet photosensitizers, and a factor of 2/5 of the best values of Φ_{NUCPL} for CdSe and Si QD light absorbers.(28-30) For this optimal Φ_{NUCPL}, an average of five 9-anthracene carboxylic acid (9-ACA) are attached on the QDs surface as a transmitter ligand. 9-ACA serves to enhance the Dexter energy transfer of triplets from the QD donor to the DPA acceptor. As summarized in Table 2, when these nanocrystals are functionalized with 9-ACA, the presence of a ZnS shell increases the band edge PLQY 26-fold from 0.59% to 15.6%. As described in Section 5 in the SI, the ZnSe/InP and ZnSe/InP/ZnS QDs were ligand exchanged with 9-ACA and redispersed in 3 mM 9,10-diphenylanthracene (DPA) in toluene solution for photon upconversion. Figure S6 shows the upconversion photoluminescence spectra for both ZnSe/InP and ZnSe/InP/ZnS samples as the concentration of the 9-ACA ligands are varied. The photon upconversion QY increases as the surface density of 9-ACA increases, then decreases after an optimum loading of 5 probably due to transmitter ligand aggregation and hence triplet excimer formation on the QD surface.

Table 2. Key Parameters of InP NCs used in upconversion and transient absorption experiments.

Sample	Ave. 9-ACA[a]	PLQY[b] (%)	UCQY[c] (%)	k_{TET}[d] (ns^{-1})
ZnSe/InP//9-ACA	5.3	0.59	4.16	0.161
ZnSe/InP/ZnS//9-ACA	5.0	15.6	4.00	0.052

[a]The average number of surface bond 9-ACA transmitter molecules per QD, obtained from UV-Vis absorbance spectra in Figure S5c. [b]Band edge PLQY with DCM standard. [c]UCQY is the measured TTA based photon upconversion emission quantum yield. 50% is defined as the maximum value of UCQY. [d]k_{TET} is the triplet energy transfer rate from NCs to 9-ACA ligands from transitnt absorpion. All measurements were at RT in toluene except for DCM in methanol.

Nanosecond transient absorption (ns-TA) spectroscopy was performed on the samples with the highest photon upconversion QYs. Ns-TA spectra associated with ZnSe/InP, ZnSe/InP/ZnS, ZnSe/InP//9-ACA and ZnSe/InP/ZnS//9-ACA at early times (4−350 ns) and at late times (500 ns−10 μs) at 350-520 nm are shown in Fig. 2, while spectra in the NIR wavelengths are in Fig. S7. All four samples are photoexcited with 532 nm (see SI for details). 532 nm does not excite the 9-ACA on the QD surface. ZnSe and ZnS have a steady

state absorption blue of 400nm (e.g. 373 nm for ZnSe in Fig S1), but our nanosecond TA spectra do not show any features from the zinc chalcogenides (Figure S8). This is likely due to the fact that thermalization occurs on the sub-ps timescale, and that 532nm photons might not be energetically able to create band edge excitons associated with the ZnSe core and ZnS shell. In comparison, Sousa et al showed that excitation of InP/ZnSe core/shell NCs with a 120 fs pump pulse centered at 480nm resolved the trajectory of an electron excited from the InP valence band to the ZnSe conduction band. Subsequently, they show that this electron relaxes to the InP conduction band from the ZnSe conduction band.(25)

Triplet exciton transfer from the InP-based QDs to the surface bound 9-ACA molecule is clearly visible from the TA spectra. After adding an average of five 9-ACA ligands to the surface, the lifetimes of both NCs are around 8 times shorter (Table 1 and Fig. 3). In other words, the presence of 9-ACA leads to the faster recovery of the GSB, indicating that 9-ACA depletes the QD exciton. Note that the ns-TA spectra from 540−1000 nm in Fig. S7 do not show any evidence for 9-ACA radical formation. The 9-ACA triplet excited state absorption (ESA) with maxima at 435 nm is observed in Fig. 2f and 2h from 500 ns for ZnSe/InP//9-ACA and ZnSe/InP/ZnS//9-ACA respectively. This indicates TET occurs from ZnSe/InP or ZnSe/InP/ZnS to the 9-ACA ligand. Fig. 4 plots the kinetics of this 9-ACA triplet ESA where the ns-TA signal from 435–440nm is averaged. As seen in Fig. 2a, 2c and 4, these wavelengths represent an isobestic point where there is little TA signal for both NCs without the 9-ACA ligand. Therefore, the rate of TET from NC to 9-ACA, is calculated from the rise in the kinetic traces in Fig. 4 using Eq. 1.

$$\left[{}^3 9-ACA\right] = \left\{1 - e^{-t/\tau_{TET}}\right\} \qquad \text{Eq. 1}$$

k_{TET} = 0.052 ns^{-1}for ZnSe/InP/ZnS is three times slower than k_{TET} = 0.16 ns^{-1} for ZnS/InP NCs without a ZnS shell (Table 1). This indicates that the ZnS shell forms a barrier to TET from the QDs to the 9-ACA ligands. The ns-TET time constants of 6–19 ns here are close to that previously reported for InP-based QDs.(12, 13) From Fig. 4, we can fit the 9-ACA triplet lifetime from the decay in exciton kinetics using Eq. 2:

$$\left[{}^3 9-ACA\right] \propto e^{-t/\tau_T} \qquad \text{Eq. 2}$$

Addition of the ZnS shell increases the 9-ACA triplet lifetime from 138 µs to 451 µs. Even though the shell growth increases the molecular triplet lifetime by removing surface trap states, it decreases k_{TET} by a factor of 3. The net result is that the photon upconversion QY is about the same for NCs with and without the two ML ZnS shell.

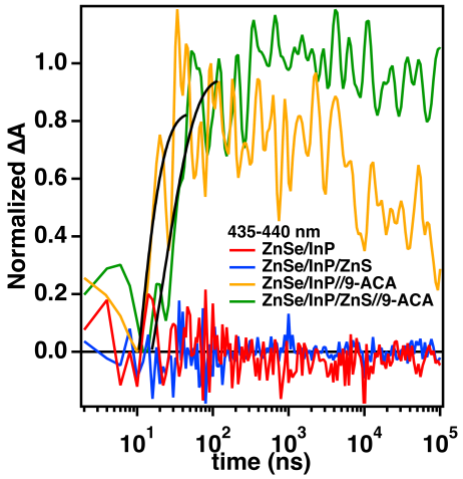

Figure 4. 9-ACA T_1 to T_n excited state absorption is shown at 435-440 nm for both ZnSe/InP//9-ACA (orange) and ZnSe/InP/ZnS//9-ACA (green) compared to NCs without 9-ACA (red: ZnSe/InP, blue: ZnSe/InP/ZnS). Fits to these kinetic traces to get k_{TET} are shown in black lines from Eq. 1.

Discussion

Our previous work shows that a sub monolayer of CdS on a PbS QD photosensitizer enhances NIR to yellow photon upconversion by suppressing undesirable hole transfer processes at the surface of the QD that deplete the exciton.(31) The best-performing PbS/CdS core/shell triplet photosensitizer that gave the highest UCQY had a 1–2Å thick CdS shell. This sub-monolayer CdS shell passivated the trap states on the QD surface. In line with our previous results, this two monolayer outer ZnS shell does suppress the deleterious surface trap states and increases the band edge emission. Unfortunately, it also presents a tunneling barrier for triplet excitons to migrate from InP to the surface bound 9-ACA: the UCQY doesn't increase for our samples with a ZnS shell. Interestingly, the threshold intensity for the transition between the quadratic and linear regime in the power dependence is lower with the ZnS shell by a factor of 2 (600 mW/cm^2 compared to 1200mW/cm^2, Figure S9). A lower threshold intensity could be caused by either a higher absorption coefficient of the NCs with a ZnS shell, or more efficient triplet energy transfer. (32, 33) Considering that the bandedge PLQY of ZnSe/InP/ZnS//9-ACA surpasses the upconversion photoluminescence QY by a factor of four (see Fig. S10 for a photograph comparing the PL), and the rate of TET is lower with the ZnS shell, our results suggest that the ZnS shell increases the extinction coefficient of the QDs. This is not surprising because the size of the QDs increase from 4.6 nm to 5.8 nm in diameter with the ZnS shell.

Conclusion

Single component InP NCs are not used in any commercial applications because of broad ensemble photoluminescence (PL) linewidths and low PL quantum yields. Core-shell heterostructures have been used to mitigate the deleterious effects of surface dangling bonds on the optoelectronic properties of InP-based NCs. The ZnSe/InP/ZnS heterostructure here is promising because the InP inner shell thickness can be tuned to induce absorption in the NIR window.(9) The ZnS outer shell thickness can be synthetically controlled to passivate surface traps and increase transmitter triplet lifetime. The work here provides a roadmap to using QD-based light absorbers for the conversion of NIR to blue light for biological imaging.

Supporting Information

Additional experimental details, materials, and methods, including photographs of experimental setup.

Acknowledgments

We would like to acknowledge salary support from the National Science Foundation (IIP-2147791); and Air Force of Scientific Research award FA9550-20-1-0112 for instrumentation. We thank Diego Fernandez from the Univ. of Utah ICP-MS Metals and Strontium Isotope Facility for performing ICP measurements and Odin Achorn for his guidance on the initial synthesis of InP/ZnSe via his variable rate injection method.

References

[1] T. Kim, K.-H. Kim, S. Kim, S.-M. Choi, H. Jang, H.-K. Seo, H. Lee, D.-Y. Chung, E. Jang Efficient and Stable Blue Quantum Dot Light-Emitting Diode, *Nature*, **2020** *586* 385-389.

[2] E. Jang, Y. Kim, Y.-H. Won, H. Jang, S.-M. Choi Environmentally Friendly Inp-Based Quantum Dots for Efficient Wide Color Gamut Displays, *ACS Energy Letters*, **2020** *5* 1316-1327.

[3] Y.-H. Won, O. Cho, T. Kim, D.-Y. Chung, T. Kim, H. Chung, H. Jang, J. Lee, D. Kim, E. Jang Highly Efficient and Stable Inp/Znse/Zns Quantum Dot Light-Emitting Diodes, *Nature*, **2019** *575* 634-638.

[4] W. Shen, H. Tang, X. Yang, Z. Cao, T. Cheng, X. Wang, Z. Tan, J. You, Z. Deng Synthesis of Highly Fluorescent Inp/Zns Small-Core/Thick-Shell Tetrahedral-Shaped Quantum Dots for Blue Light-Emitting Diodes, *Journal of Materials Chemistry C*, **2017** *5* 8243-8249.

[5] H. Zhang, X. Ma, Q. Lin, Z. Zeng, H. Wang, L.S. Li, H. Shen, Y. Jia, Z. Du High-Brightness Blue Inp Quantum Dot-Based Electroluminescent Devices: The Role of Shell Thickness, *The Journal of Physical Chemistry Letters*, **2020** *11* 960-967.
[6] J. Lim, M. Park, W.K. Bae, D. Lee, S. Lee, C. Lee, K. Char Highly Efficient Cadmium-Free Quantum Dot Light-Emitting Diodes Enabled by the Direct Formation of Excitons within Inp@Znses Quantum Dots, *ACS Nano*, **2013** *7* 9019-9026.
[7] D.H. Atha, A. Nagy, A. Steinbrück, A.M. Dennis, J.A. Hollingsworth, V. Dua, R. Iyer, B.C. Nelson Quantifying Engineered Nanomaterial Toxicity: Comparison of Common Cytotoxicity and Gene Expression Measurements, *Journal of Nanobiotechnology*, **2017** *15*.
[8] P.M. Allen, W. Liu, V.P. Chauhan, J. Lee, A.Y. Ting, D. Fukumura, R.K. Jain, M.G. Bawendi Inas(Zncds) Quantum Dots Optimized for Biological Imaging in the near-Infrared, *Journal of the American Chemical Society*, **2010** *132* 470-471.
[9] A.M. Saeboe, A.Y. Nikiforov, R. Toufanian, J.C. Kays, M. Chern, J.P. Casas, K. Han, A. Piryatinski, D. Jones, A.M. Dennis Extending the near-Infrared Emission Range of Indium Phosphide Quantum Dots for Multiplexed in Vivo Imaging, *Nano Lett*, **2021** *21* 3271-3279.
[10] S.L. Jacques Optical Properties of Biological Tissues: A Review, *Physics in Medicine & Biology*, **2013** *58* 5007-5008.
[11] E. Cassette, M. Helle, L. Bezdetnaya, F. Marchal, B. Dubertret, T. Pons Design of New Quantum Dot Materials for Deep Tissue Infrared Imaging, *Adv Drug Deliv Rev*, **2013** *65* 719-731.
[12] X. Zhang, M.H. Hudson, F.N. Castellano Engineering Long-Lived Blue Photoluminescence from Inp Quantum Dots Using Isomers of Naphthoic Acid, *Journal of the American Chemical Society*, **2022** *144* 3527-3534.
[13] R. Lai, Y. Sang, Y. Zhao, K. Wu Triplet Sensitization and Photon Upconversion Using Inp-Based Quantum Dots, *Journal of the American Chemical Society*, **2020** *142* 19825-19829.
[14] P. Ramasamy, N. Kim, Y.-S. Kang, O. Ramirez, J.-S. Lee Tunable, Bright, and Narrow-Band Luminescence from Colloidal Indium Phosphide Quantum Dots, *Chem. Mat.*, **2017** *29* 6893-6899.
[15] P. Ramasamy, K.-J. Ko, J.-W. Kang, J.-S. Lee Two-Step "Seed-Mediated" Synthetic Approach to Colloidal Indium Phosphide Quantum Dots with High-Purity Photo- and Electroluminescence, *Chem. Mat.*, **2018** *30* 3643-3647.
[16] M.D. Tessier, E.A. Baquero, D. Dupont, V. Grigel, E. Bladt, S. Bals, Y. Coppel, Z. Hens, C. Nayral, F. Delpech Interfacial Oxidation and Photoluminescence of Inp-Based Core/Shell Quantum Dots, *Chem. Mat.*, **2018** *30* 6877-6883.
[17] Z. Xu, Y. Li, J. Li, C. Pu, J. Zhou, L. Lv, X. Peng Formation of Size-Tunable and Nearly Monodisperse Inp Nanocrystals: Chemical Reactions and Controlled Synthesis, *Chem. Mat.*, **2019** *31* 5331-5341.
[18] R.T. Lechner, G. Fritz-Popovski, M. Yarema, W. Heiss, A. Hoell, T.U. Schülli, D. Primetzhofer, M. Eibelhuber, O. Paris Crystal Phase Transitions in the Shell of Pbs/Cds Core/Shell Nanocrystals Influences Photoluminescence Intensity, *Chem. Mat.*, **2014** *26* 5914-5922.
[19] S.M. Geyer, J.M. Scherer, N. Moloto, F.B. Jaworski, M.G. Bawendi Efficient Luminescent Down-Shifting Detectors Based on Colloidal Quantum Dots for Dual-Band Detection Applications, *ACS Nano*, **2011** *5* 5566-5571.
[20] D.C.J. Neo, C. Cheng, S.D. Stranks, S.M. Fairclough, J.S. Kim, A.I. Kirkland, J.M. Smith, H.J. Snaith, H.E. Assender, A.A.R. Watt Influence of Shell Thickness and Surface Passivation on Pbs/Cds Core/Shell Colloidal Quantum Dot Solar Cells, *Chem. Mat.*, **2014** *26* 4004-4013.

[21] M. Montalti, A. Credi, L. Prodi, M.T. Gandolfi Handbook of Photochemistry, **2006**.
[22] O.B. Achorn, D. Franke, M.G. Bawendi Seedless Continuous Injection Synthesis of Indium Phosphide Quantum Dots as a Route to Large Size and Low Size Dispersity, *Chem. Mat.*, **2020** *32* 6532-6539.
[23] M.E. Mundy, F.W. Eagle, K.E. Hughes, D.R. Gamelin, B.M. Cossairt Synthesis and Spectroscopy of Emissive, Surface-Modified, Copper-Doped Indium Phosphide Nanocrystals, *ACS Materials Letters*, **2020** *2* 576-581.
[24] J.J. Li, Y.A. Wang, W. Guo, J.C. Keay, T.D. Mishima, M.B. Johnson, X. Peng Large-Scale Synthesis of Nearly Monodisperse Cdse/Cds Core/Shell Nanocrystals Using Air-Stable Reagents Via Successive Ion Layer Adsorption and Reaction, *Journal of the American Chemical Society*, **2003** *125* 12567-12575.
[25] F. Sousa Velosa, H. Van Avermaet, P. Schiettecatte, L. Mingabudinova, P. Geiregat, Z. Hens State Filling and Stimulated Emission by Colloidal Inp/Znse Core/Shell Quantum Dots, *Advanced Optical Materials*, **2022** *10*.
[26] E.M. Janke, N.E. Williams, C. She, D. Zherebetskyy, M.H. Hudson, L. Wang, D.J. Gosztola, R.D. Schaller, B. Lee, C. Sun, et al Origin of Broad Emission Spectra in Inp Quantum Dots: Contributions from Structural and Electronic Disorder, *Journal of the American Chemical Society*, **2018** *140* 15791-15803.
[27] A.T. Nguyen, P. Cavanaugh, I.J.-L. Plante, C. Ippen, R. Ma, D.F. Kelley Auger Dynamics in Inp/Znse/Zns Quantum Dots Having Pure and Doped Shells, *The Journal of Physical Chemistry C*, **2021** *125* 15405-15414.
[28] Z. Huang, Z. Xu, M. Mahboub, Z. Liang, P. Jaimes, P. Xia, K.R. Graham, M.L. Tang, T. Lian Enhanced near-Infrared-to-Visible Upconversion by Synthetic Control of Pbs Nanocrystal Triplet Photosensitizers, *Journal of the American Chemical Society*, **2019** *141* 9769-9772.
[29] E.M. Rigsby, T. Miyashita, P. Jaimes, D.A. Fishman, M.L. Tang On the Size-Dependence of Cdse Nanocrystals for Photon Upconversion with Anthracene, *The Journal of Chemical Physics*, **2020** *153* 114702.
[30] P. Xia, J. Schwan, T.W. Dugger, L. Mangolini, M.L. Tang Air-Stable Silicon Nanocrystal-Based Photon Upconversion, *Advanced Optical Materials*, **2021** *9* 2100453.
[31] Z. Huang, Z. Xu, M. Mahboub, X. Li, J.W. Taylor, W.H. Harman, T. Lian, M.L. Tang Pbs/Cds Core–Shell Quantum Dots Suppress Charge Transfer and Enhance Triplet Transfer, *Angewandte Chemie International Edition*, **2017** *56* 16583-16587.
[32] A. Monguzzi, R. Tubino, S. Hoseinkhani, M. Campione, F. Meinardi Low Power, Non-Coherent Sensitized Photon up-Conversion: Modelling and Perspectives, *Phys Chem Chem Phys*, **2012** *14* 4322-4332.
[33] A. Monguzzi, M. Mauri, M. Frigoli, J. Pedrini, R. Simonutti, C. Larpent, G. Vaccaro, M. Sassi, F. Meinardi Unraveling Triplet Excitons Photophysics in Hyper-Cross-Linked Polymeric Nanoparticles: Toward the Next Generation of Solid-State Upconverting Materials, *The Journal of Physical Chemistry Letters*, **2016** *7* 2779-2785.

TOC Graphic


InP inner shell
· Light absorber
Photon
upconversion
ZnS outer shell
· Passivate
surface traps
· Increase
transmitter
triplet lifetime
ZnSe
InP
ZnS
O
O